Transforming a Simple Commercial Glue into Highly Robust Superhydrophobic Surfaces *via* Aerosol Assisted Chemical Vapour Deposition

Aoyun Zhuang[a, b], Ruijin Liao[a, *], Yao Lu[c], Sebastian C. Dixon[b], Arreerat Jiamprasertboon[b, d], Faze Chen[b], Sanjayan Sathasivam[b], Ivan P. Parkin[b] and Claire J. Carmalt[b, *]

[a] State Key Laboratory of Power Transmission Equipment & System Security and New Technology, Chongqing University, Chongqing 400044, China

[b] Department of Chemistry, University College London, London, WC1H 0AJ, United Kingdom

[c] Nanoengineered Systems Laboratory, UCL Mechanical Engineering, University College London, London, WC1E 7JE, United Kingdom

[d] School of Chemistry, Institute of Science, Suranaree University of Technology, 111 University Avenue, Muang, Nakhon Ratchasima, 30000, Thailand

*Corresponding author, E-mail: rjliao@cqu.edu.cn, E-mail: c.j.carmalt@ucl.ac.uk Tel.: +44 (0) 20 7679 4637

Keywords: Glue, Robust, Dynamic temperature, Superhydrophobicity, AACVD.

Abstract

Robust superhydrophobic surfaces were synthesised as composites of the widely commercially available adhesives epoxy resin (EP) and polydimethylsiloxane (PDMS). The EP layer provided a strongly adhered micro/nano-scale structure on the substrates, while the PDMS was used as a post-treatment to lower the surface energy. In this study, the depositions of EP films were taken at a range of temperatures, deposition times and substrates via aerosol-assisted chemical vapour deposition (AACVD). A novel dynamic deposition temperature approach was developed to create multiple-layered periodic micro-nano structures which significantly improved the surface mechanical durability. Water droplet contact angles (CA) of 160° were observed with droplet sliding angles (SA) frequently <1°. Rigorous sandpaper abrasion test demonstrated retention of superhydrophobic properties and superior robustness therein, while wear, anti-corrosion (pH = 1 - 14, 72 h) and UV testing (365 nm, 3.7 mW/cm^2, 120 h) were carried out to exhibit the environmental stability of the films. Self-cleaning behaviour was demonstrated in clearing the surfaces of various contaminating powders and aqueous dyes. This facile and flexible method for fabricating highly durable superhydrophobic polymer films points to a promising future for AACVD in their scalable and low-cost production.

1. Introduction

Inspired by the natural surfaces of many animals and plants, one famous example of which is the Lotus leaf,[1–3] superhydrophobic surfaces constitute an exciting field of scientific research due to their self-cleaning, anti-corrosion, drag reduction, oil-water separation and icephobic functional properties.[4–6] Synthetic routes to superhydrophobic surfaces generally involve two steps, the first being the physical introduction of micro/nano-structured surface roughness, followed by chemical treatment to yield a low-energy surface.[7–9] Superhydrophobic surface fabrication can be achieved by

a number of common lab-scale methods such as laser etching, sol-gel deposition and electrospinning[10–14]. However, limitation to industrial scalability is one drawback that each of these methods have in common. They either need strict conditions, sophisticated equipment or are simply intrinsically limited. In recognition of this issue, numerous reports have arisen of more budget- or scale-friendly approaches;[15–17] Seo *et al.* used a candle wax-coated surface followed by addition of soot from a candle flame to yield a superhydrophobic surface.[18] Latthe *et al.* sprayed a nanoparticle dispersion onto a surface to achieve the same.[19] Though conceptually facile, the materials deposited possessed limited adhesive force to their substrates, yielding poor mechanical stabilities therein.

As a result of this, the deposition of robust superhydrophobic surfaces has lately been a prolific field of research.[20–22] Hashian *et al.* reported a nano-replication process consisting of metal nano-structuring stages of acid etching, atomic layer deposition (ALD) of a TiO_2 layer finished with polymer replication.[23] Gong and co-works have used a femtosecond laser-ablated template to fabricate robust and stable transparent superhydrophobic polydimethylsiloxane films.[24] Although the superhydrophobic coatings reported in these studies appeared robust, the methods used in their preparation limited their applicability.

As such, there has been a shift towards fabricating robust superhydrophobic surfaces by methods which are uncomplicated and flexible in their applicability. Robust self-cleaning surfaces were deposited with success by Lu *et al.* on various substrates from an ethanolic colloid containing perfluorosilane-coated TiO_2 nanoparticles.[25] Si *et al.* have used an omnipotent epoxy resin coating prepared with stearic acid-capped $Mg(OH)_2$ powder to fabricate superhydrophobic coatings via an antideposition route with a hydrophobisation step.[26] Zhang and co-workers introduced an immersion method to prepare a hierarchically-structured flowerlike ZnO/epoxy resin composite coating featuring self-healing capability.[27] In these methods, the recurring trend is that nanoparticles and adhesives are widely used in superhydrophobic surface fabrication in which the former provides roughness while the latter provides a strong bond between the nanoparticles and the substrate.

Epoxy resin is an excellent adhesive and commercially available; it has been widely utilised as a cross-linking agent to bond nanoparticles or nanotubes to create micro/nano structures that are required by superhydrophobic coatings.[26–28] However, the bonding behaviour is subject to the interactions between epoxy resin and nanoparticles/nanotubes, and this greatly limits the mechanical durability of superhydrophobic surfaces.[29,30] Fabrication of superhydrophobic surfaces using just the adhesive alone would avoid a weak interaction between polymer and nanoparticles so that the mechanical robustness could be further improved, however, such a method has been scarcely reported.

Aerosol-assisted chemical vapour deposition (AACVD) is a simple variant of CVD, in which a solution containing the material precursors is delivered to the CVD reactor as an aerosol generated by an ultrasonic atomiser. Precursors for AACVD need only be soluble in suitable media; this gives AACVD a distinct advantage over traditional CVD methods in terms of precursor availability. It has demonstrated success in preparing myriad materials including n-type ZnO, TiO_2, GaAs, BiOX (where X = Cl, Br, I) and SnO_2 : F suiting many useful functional purposes.[31–33] Likewise it has been used in the preparation of numerous polymer films.[34–37]

In this paper, we use the unique AACVD method to deposit coatings of epoxy resin from a vapour-phase stream of the aerosolised precursor towards the heated glass substrate. This method confers a hierarchical micro/nano-scopically rough structure to the epoxy resin coating, enabling superhydrophobicity upon post-treatment with PDMS while the adhesive strength of the epoxy resin on the glass confers its mechanical durability. The mechanical robustness of the superhydrophobic coatings was significantly improved by introducing a "three-layered" film using the dynamic temperature approach. The robust "three-layered" superhydrophobic coatings retained their superhydrophobicity even after 100 cycles of peeling tape test, UV exposure for 120 h, strong acid/base soak for 72 h and severe sand paper abrasion for 5 m.

2. Experimental

2.1. Materials

Araldite® 506 epoxy resin and triethylenetetramine (technical grade, 60%) were purchased from Sigma-Aldrich, UK. The PDMS elastomer precursor and its curing agent, Sylgard-184, were bought from Univar Specialty Consumables. Organic solvents, including methanol and ethyl acetate, were purchased from Fisher Scientific UK and used as supplied. Standard microscope glass slides were purchased from VWR International, Inc. Silicon wafers were purchased from Nova Electronics Materials, TX, USA. Other substrates, including aluminium, copper and stainless steel were purchased from Hecheng Hardware Ltd. Micro-grained sandpaper (TUFBAK, ADALOX, P1000) was bought from Norton Company. The sand grains for testing the resistance of abrasion wear were bought from VWR International, Inc. Activated carbon powder was supplied by Fisher Scientific UK. Congo red, Trypan blue and Titan yellow dye were supplied by BDH Chemicals Ltd.

2.2. Fabrication

2.2.1 EP films deposited on different substrates at various fixed temperatures and durations

Araldite® 506 epoxy resin and triethylenetetramine (1.0 g : 0.1 g) were combined and dissolved in methanol (20 mL). The EP film depositions on different substrates were operated using a cold-walled horizontal-bed CVD reactor.[37] The reactor was assembled in a top-down heating configuration, with the carbon heating block positioned above a plate (14.5 cm × 4.5 cm × 0.4 cm) supporting the substrates (glass, silicon, aluminium, stainless steel or copper). The distance between the carbon block and the substrate was 8 mm. A quartz tube was used to enclose the carbon block and substrates. Upon reaching the set reactor temperature (290 °C, 310 °C, 330 °C or 350 °C), a precursor aerosol was generated by a ultrasonic humidifier (PIFCO, 25 W, 40 kHz), and then the aerosol was transported to the heated substrate with N_2 (0.5 L/min). And the EP film depositions were carried out for various durations (2 min, 5 min, 8 min or 40 min), and then the substrates coated with EP films were handled in air after cooling under nitrogen.

2.2.2 Low surface energy treatment

The PDMS elastomer precursor and its curing agent (1.0 g : 0.1 g), Sylgard-184, were combined and dissolved in ethyl acetate (50 mL) with stirring. The as-prepared EP films were immersed into the silicone elastomer and curing agent solution at ambient temperature for 5 min and then heated at 250 °C for 5 min, finally yielding the superhydrophobic epoxy resin/polydimethylsiloxane (EP/PDMS) film.

2.2.3 EP films deposited at dynamic temperature

In a variant of 2.2.1, the reactor temperature was set to 290 °C and the deposition commenced, at which point the temperature was set to increase from 290 °C to 350 °C during the deposition at a rate of 2 °C /min. Once the entire EP precursor (20 mL) had been aerosolised, the reactor temperature was cooled back down to 290 °C and the process repeated again with the dynamic temperature control for a second and third EP layer, finally yielding the three-layered robust EP film. The same process of the low surface energy treatment in 2.2.2 was applied to the three-layered robust EP film to yield the robust, superhydrophobic three-layered EP/PDMS film.

2.3. Characterisation

The morphology images of the as-prepared samples were observed using a scanning electron microscope (SEM, JEOL JSM-6301F). A thin gold layer was sputtered onto the sample surfaces under vacuum to improve the electrical conductivity. ATR-FTIR (Attenuated total reflection Fourier transform infrared spectroscopy) measurement was taken from 400 to 3600 cm^{-1} using a Perkin-Elmer Spectrum-100 (Ge crystal) equipped with a universal ATR attachment. UV-vis spectra measurements were taken from 350 to 800 nm using a Perkin Elmer Lambda 950 UV/VIS spectrometer single beam instrument. A drop shape instrument (FTA-1000) was used to test the water CA; the volume of the water droplet was 5 μL. The tilted drop method was used to test the sliding angle (SA), and the volume of the water droplet was 15 μL. At least 6 different positions on each sample were tested. The water droplet bouncing on the superhydrophobic EP/PDMS surfaces was recorded using a high-speed camera (Phantom v411, Vision Research, Inc.).

2.4 Mechanical robustness testing

A sandpaper abrasion test was used to demonstrate the robustness of EP/PDMS films fabricated under both a fixed temperature (350 °C) and dynamic temperature (290 °C - 350 °C). A 26 × 26 mm sample was placed onto the sandpaper with the EP/PDMS film touching the sandpaper, and then a 100 g weight was put on the middle of the sample. The sample was moved 25 cm across the sandpaper by an external force parallel to the substrate. The sample was rotated 90° clockwise after each abrasion to make the sample abrade from all four directions. The CAs, SAs and SEM images of the samples were taken after abrasion tests.

2.5 Atmospheric durability testing

To investigate the durability of the three-layered superhydrophobic EP/PDMS film, a set of tests were carried out including wear resistance, tape peeling test, UV resistance and anti-corrosion test, whereby the resultant changes in CAs and SAs for the surfaces were taken as a metric to demonstrate the retention of superhydrophobic behaviour. Wear resistance of the EP/PDMS film was tested by dropping 3000 water droplets (~ 15 μL) and 20 g of sand grains onto the sample surface from set heights (20 cm - 80 cm). Tape peeling test was used to investigate the adhesion between superhydrophobic EP/PDMS films and the substrates, and the CAs, SAs and weight of the sample were measured after each 20-cycle. In order to test for UV resistance, the samples were exposed to UV light (365 nm, 3.7 mW/cm^2) for 120 h at room temperature, and the CAs and SAs were measured at each 24-hour period. The anti-corrosion test was performed by immersing the samples in acidic (HCl) and basic (NaOH) aqueous solutions (pH = 1 - 14) for 72 h.

2.6 Self-cleaning functional testing

Self-cleaning properties were investigated as follows: activated carbon powder and various dye powders including Congo red, Trypan blue and Titan yellow were chosen as representative examples of contaminant to be dispersed on the EP/PDMS film. Then, the EP/PDMS surfaces were impinged by water droplets to wash away the contaminant. To test the self-cleaning property under corrosive liquid, acidic (HCl, pH = 1) and basic (NaOH, pH = 14) aqueous solution were dropped onto the surface to wash away the activated carbon powder from the EP/PDMS surface. Congo red, Trypan blue and Titan yellow aqueous dyes were also used in further testing of the self-cleaning property.

3. Results and discussion

3.1 Microscopy, wettability and composition

EP/PDMS composite films grown using a fixed EP deposition temperature of 350 °C were fabricated on five different material substrates including glass, silicon, aluminium, stainless steel and copper. The films covered the substrates totally and were well adhered due to the excellent bonding strength between epoxy resin and various material substrates. Fig. 1(a) shows the optical photographs and the CAs of water droplets dyed with methylene blue on the bare substrates and corresponding EP/PDMS-coated substrates. It can be clearly observed that the hydrophobic properties of different substrates were significantly improved after coating with the EP/PDMS films.

Scanning electron micrographs (SEM) of the EP/PDMS film on the glass substrate, as depicted in Fig. 1(b), showed how the hierarchical micro- and nano-sized spherical particles distributed across the surface constituted the rough morphology of the superhydrophobic EP/PDMS film. At higher magnification shown in Fig. 1(c), it can be observed that much of the particle size distribution lay in the 200 nm - 2 μm range. Smaller nanoscopic particles protruded from the micro-structure (diameter: 200 - 300 nm), likely making a significant contribution to superhydrophobicity.[38] Hierarchical micro-/nano-scaled structure encourages air-trapping beneath water droplets as per the Cassie-Baxter model, resulting in larger contact angles.

Fig. 1(d) shows the FTIR spectrum of the superhydrophobic EP/PDMS film. The observed peaks assigned in the figure correspond to the vibrations of molecular bonds of both epoxy resin and PDMS as follows. The bands at 3059 cm^{-1}, 1606 cm^{-1}, 1506 cm^{-1}, 1030 cm^{-1} and 936 cm^{-1} were assigned to the stretching mode of C-H (oxirane ring), C=C (aromatic ring), C-C (aromatic ring), C-O-C (oxirane ethers) and C-O (oxirane group) for epoxy resin.[39] Regarding PDMS, the bands at 2963 cm^{-1} and 1294 cm^{-1} were assigned to asymmetric CH_3 stretching and CH_3 deformation in Si-CH_3. The peaks of 1030 cm^{-1} and 1011 cm^{-1} were assigned to Si-O-Si stretching. Moreover, the peak at 826 cm^{-1} was assigned to CH_3 rocking and Si-C stretching in Si-CH_3.[40]

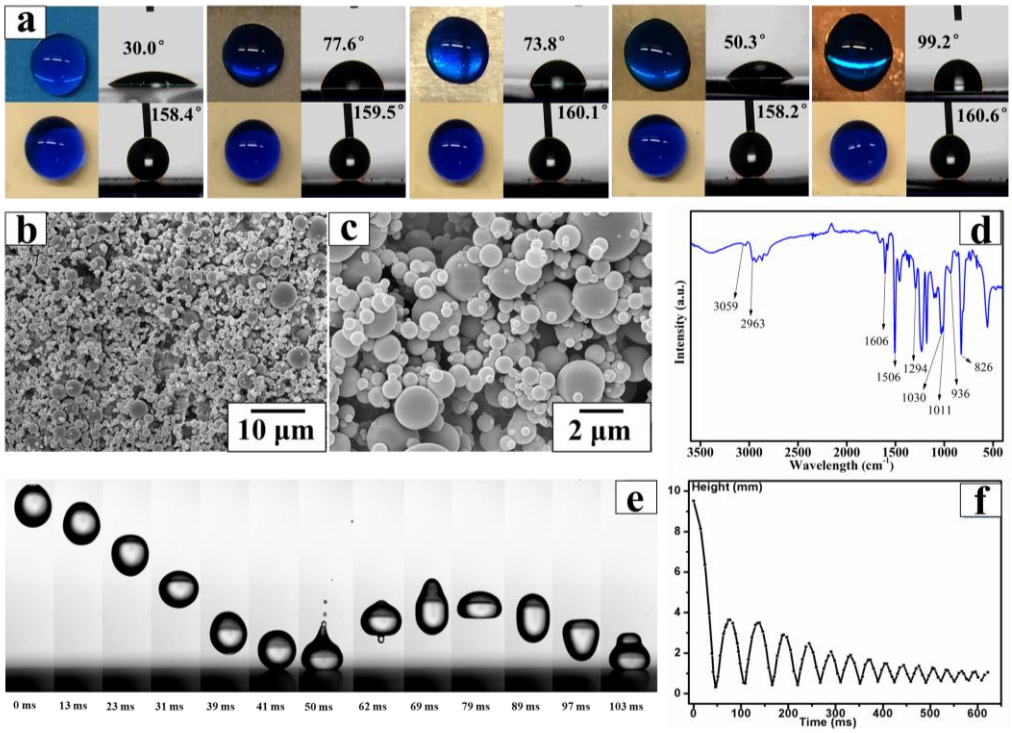

Fig. 1. Optical photographs of water droplets dyed with methylene blue on the different bare substrates and corresponding substrates covered with EP/PDMS films deposited on five different material substrates including glass, silicon, aluminium, stainless steel and copper (a); FE-SEM photographs of the EP/PDMS film (b) - (c); FTIR spectrum for the superhydrophobic EP/PDMS film (d); A water droplet bouncing on the superhydrophobic EP/PDMS film (e) and the height of the bouncing droplet as a function of time (f) (water drop diameter D = 2.50 mm; impact velocity V = 0.40 m/s).

Water droplet bouncing on a surface is an indication of its superhydrophobicity.[41,42] Using a high-speed camera at 3000 fps, bounce dynamics of water droplets upon the samples could be observed under ambient conditions. Photographs taken during this process (Fig. 1(e)) illustrate a water droplet being released (9.5 mm height) onto the sample. Impact of the droplet at the surface occurred at t = 41 ms with velocity 0.40 m/s. This was followed by detachment on the rebound with several smaller water droplets separating from the larger droplet. At its peak after the first bounce, the height of the droplet was 3.8 mm (t = 79 ms). Thirteen bounces were recorded in this way from a single drop, demonstrating minimal adhesion between the EP/PDMS film and the water droplets, and its superhydrophobicity therein. The full video can be seen in the online supplementary Video S1.

3.2 Effect of deposition temperature

A range of EP films were deposited on glass substrates with different fixed reactor temperatures of 290 °C, 310 °C, 330 °C and 350 °C. From the optical photographs of the EP films deposited with different temperatures on the glass substrate shown in Fig. 2(a) - (d), it can be seen that the EP film showed high transparency at the low temperature (290 °C) and the appearance of the film got thicker and whiter with higher temperatures (310 °C, 330 °C and 350 °C). As seen from the SEM images of the corresponding EP films in Fig. 2(a) - (d), it was observed that the particles of the EP film fabricated at 290 °C were globular and nearly 100 - 200 μm in diameter, which is much larger than that the spherical particles (200 nm - 2 μm) of the EP film fabricated at 350 °C. This is due to the

curing process of the EP precursor at the different temperatures. The EP precursor did not totally solidify before deposition onto the substrate at the low temperature (290 °C) and hence would deposit as liquid state, resulting in the relatively flat and smooth EP film. By contrast, the EP precursor at the higher temperature (350 °C) mostly cured prior to deposition, which could create the nano-EP particles to improve the roughness of the EP film (while reducing the transparency). From the SEM images as shown in Fig. 2(a) to (d), it can be seen that formation of nano-scale EP particles occurs to a greater degree with increasing deposition temperature, correlating with an increasing CA (109.7°, 128.6°, 157.9°, 161.0° at 290 °C, 310 °C, 330 °C, 350 °C respectively) and demonstrating the importance of roughness towards superhydrophobicity. Cassie and Baxter related wettability and surface heterogeneity by Equation 1[43]:

$$\cos\theta_c = \cos\theta - f_2(\cos\theta + 1) \quad (1)$$

, where f_2 is the fractions of air in the composite surface, θ_c and θ are contact angles on the rough and untextured surfaces, respectively. When the contact angle θ of untextured surface is constant, the higher liquid-air surface f_2 would lead to a larger contact angle θ_c of the superhydrophobic surfaces. The water contact angle of the flat PDMS film has been tested to be 108.8°. The value f_2 was calculated for the EP/PDMS films to be about 0.022, 0.445, 0.892, 0.920 at 290 °C, 310 °C, 330 °C, 350 °C respectively according to the Equation (1) which indicated that the actual fractions of contact area between solid surface and water surface was 0.978, 0.555, 0.108 and 0.080 respectively.

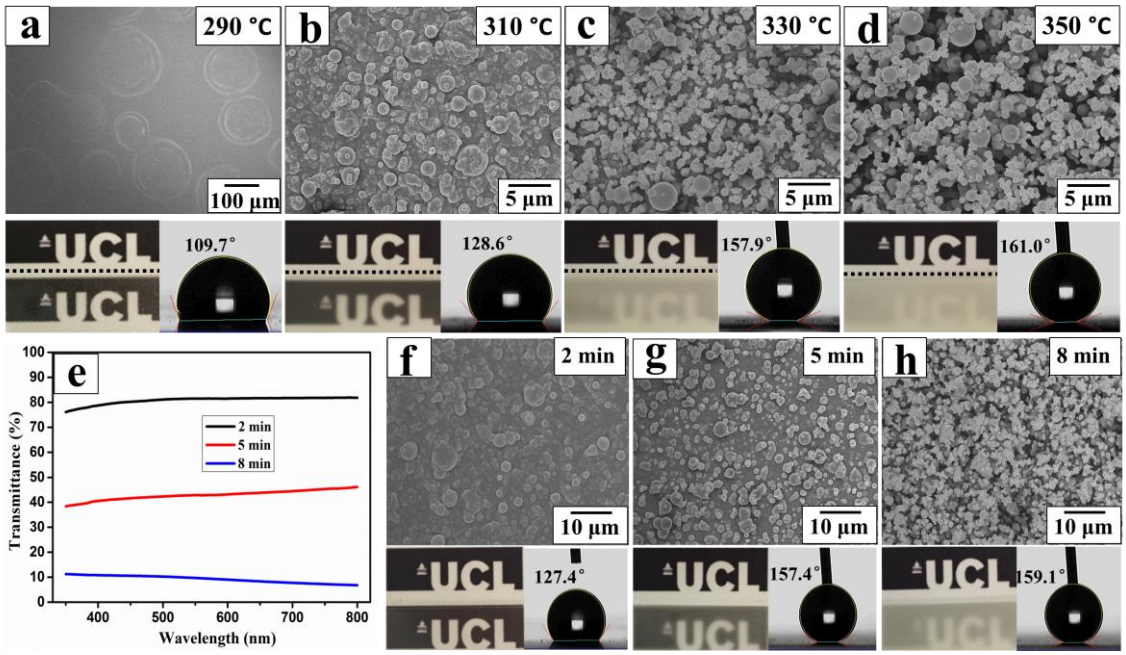

Fig. 2. SEM, transparency (see lower UCL logo in each photograph) and CA images of the EP/PDMS films fabricated at different EP deposition temperatures (a) - (d); visible transmittance as a function of the light wavelength for different deposition times (e) and SEM, transparency and CA images for EP/PDMS films fabricated with different deposition times at 350 °C (f) - (h).

To investigate the transparency of the sample films, the EP films were deposited at 350 °C with different times respectively (2 min, 5 min and 8 min). Fig. 2(e) - (h) shows transmittance, SEM,

photographs showing visible transparency and CA images for the sample EP/PDMS films with different surface structure. The sample in Fig. 2(f) grown for 2 min had the most flat film, resulting in it having the highest measured transparency (around 80% shown in Fig. 2(e)) but the lowest contact angle of 127.4°, which is not considered to be superhydrophobic.[44] The sample grown for 5 min as shown in Fig. 2(g) had a higher degree of texture than that at 2 min, leading it a higher contact angle of 157.4°, while transparency fell to 40 - 50%. Given the greatest degree of surface roughness, the sample grown for 8 min, as shown in Fig. 2(h), had a water CA of 159.1°, a little higher than that for 5 min but with a dramatic decrease in transparency to <10%. Therefore, the superhydrophobicity and transparency of the thin film are in competition and depend on the degree and density of surface texture. A lesser degree of surface morphology would achieve better transparency, but at the expense of a high water contact angle. The value f_2 was calculated for the EP/PDMS films to be about 0.421, 0.886, 0.903 respectively with different deposition times (2min, 5 min and 8 min) at 350 °C according to the Equation (1) which indicated the actual fractions of contact area between solid surface and water surface was 0.579, 0.114 and 0.097 respectively. To balance the desirable properties of transparency and superhydrophobicity, the superhydrophobic and translucent sample grown for 5 min, as shown in Fig. 2(g), can be taken as a compromise between the two, which can be applied for the practical self-cleaning applications.

3.3 Robustness of the EP/PDMS films

The mechanical robustness of the superhydrophobic films is one of the most significant properties for their widespread application in numerous instances. The dynamic temperature method was used to control the size of the EP particles deposited onto the substrate, thereby improving the robustness of the EP film. An illustration of the abrasion test used for the superhydrophobic EP/PDMS films with the sandpaper is shown in Fig. 3(a). The robustness test of the EP films fabricated at a fixed temperature (350 °C) and the dynamic temperature method (290 °C - 350 °C) is shown respectively in Fig. 3(b) - (d) and Fig. 3(e) - (g). As seen from the cross-sectional SEM of the sample film fabricated at 350 °C with 40 min (Fig. 3(b)), the film was composed of micro and nano-sized spherical particles and its thickness dropped from 61.4 μm to 10.2 μm after just 1.0 m of sandpaper abrasion, indicating that the structure of the top part of the film lacked robustness. However, even with just 10.2 μm of film remaining, superhydrophobicity was retained (CA was still measured as high as 158° and the SA was less than 3°) due to the vertical uniformity of the hierarchical micro/nano-structure throughout the thickness of the film, evident from the top-down SEM image of the film shown in Fig. 3(c). After 5 m abrasion, the film thickness dropped to 8.4 μm and its surface structure got flatter which would cause larger actual fraction of contact area between solid surface and water surface, resulting that its CA reduced to 135° shown in Fig. 3(d).

While deposition at fixed temperature yielded a vertically uniform EP film, the dynamic temperature method could produce a layered film with horizontal strata of varying roughness. The gradual increase of the deposition temperature as the reaction proceeded, as iterated in three identical stages, yielded the complex film morphology with vertically periodic roughness. As seen from the cross-sectional SEM images in Fig. 3(e), these multiple-layered periodic films were composed of a set of three repeat structures. Each stage features an amorphous, space-filling layer which grows at the beginning of the temperature ramping cycle (i.e. at around 290 °C). As the temperature increased, greater degrees of microscopic then nanoscopic structure developed atop the smoother base. Upon

completion of a single ramping cycle (i.e. once 350 °C had been reached), deposition would cease while the temperature was brought back down to 290 °C. Recommencing the deposition cycle yields a further deposition of a smooth EP layer in and amongst the existing rough structure, which then builds up into further rough structure as the deposition cycle proceeds. The effects of this can be seen in Fig. 3(e), in which there appear to be three approximate regions of continuous agglomerated EP, separated by porous layers of EP microstructure.

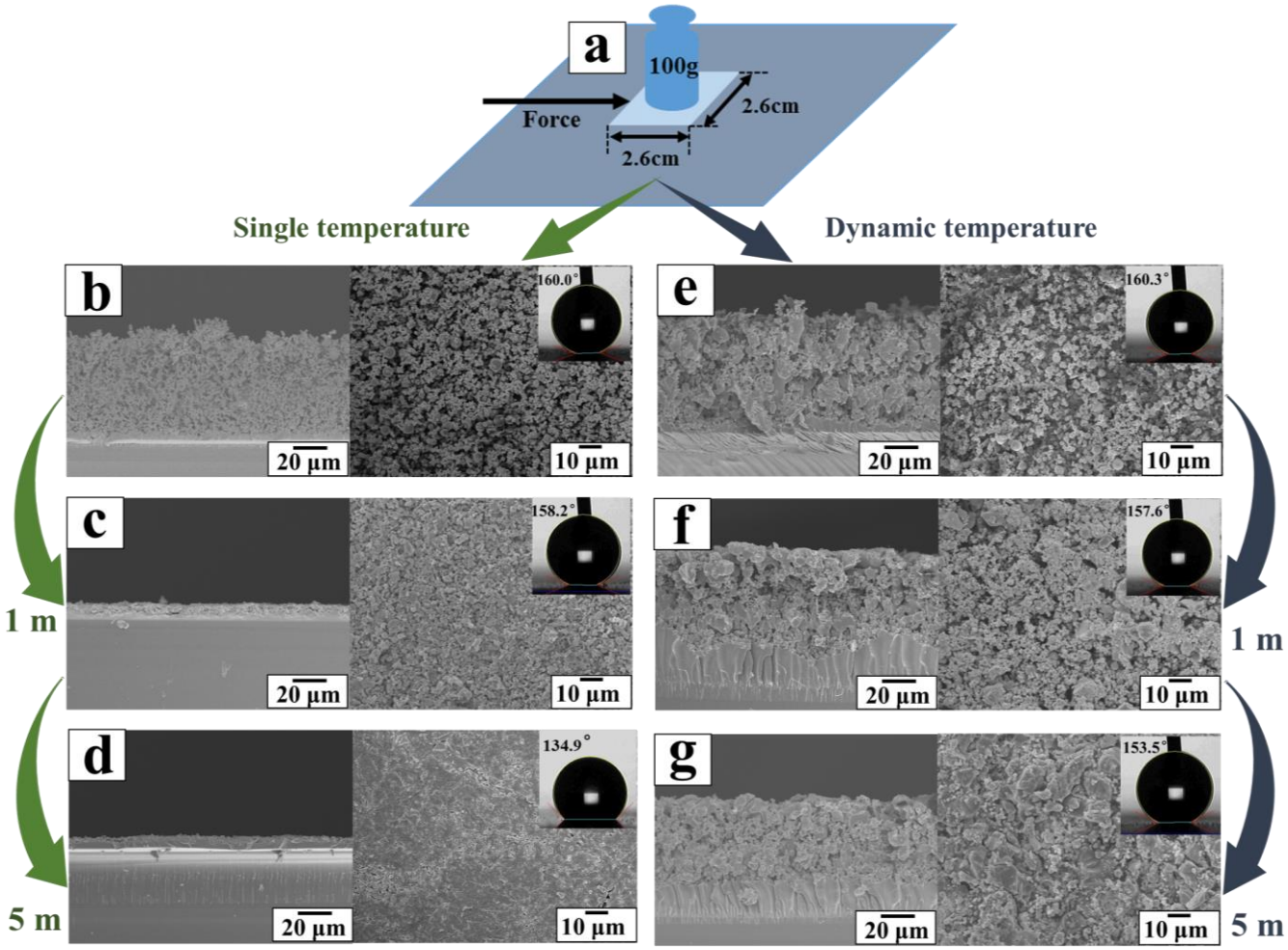

Fig. 3. Illustration of the abrasion test for EP/PDMS films with the sandpaper (a); cross-sectional, top-view SEM and contact angles of EP/PDMS films fabricated at 350 °C before (b) and after (c) 1 m abrasion and 5 m (d) abrasion; cross-sectional, top-view SEM and contact angles of the three-layered EP/PDMS films fabricated with dynamic temperature (290 - 350 °C) before (e) and after 1 m (f) abrasion and 5 m (g) abrasion.

The robustness of the three-layered EP/PDMS film was tested by the sandpaper abrasion method as shown in the online supplementary Video S2. As seen from the cross-sectional SEM shown in Fig. 3(e) and (f), the film's thickness only reduced 4.0 μm (from 84.1 μm to 80.1 μm) after 1 m abrasion, much less than that of the single-layered EP film fabricated at 350 °C. From the top-view SEM of the film after 1 m abrasion shown in Fig. 3(f), it can be seen that the surface nanostructure remained, enabling retention of superhydrophobic behaviour. Moreover, Fig. 3 (g) showed that the CA of the

film was still >153° and SA was <4° even after 5 m abrasion, demonstrating that the robustness of the three-layered EP/PDMS film was significantly improved with the dynamic temperature control method compared to the film fabricated at a fixed temperature of 350 °C.

The EP film fabricated at fixed temperature (350 °C) was mostly composed of small spherical EP particles (200 nm - 2 μm) which had formed before depositing onto the glass substrate. As a result, the particles were weakly bound to each other and resulted in the fragility of the film. But for the EP films fabricated with the dynamic temperature (290 - 350 °C), the EP precursor would not cure at the low reactor temperature (290 °C) before depositing onto the glass substrate, enabling wetting of the substrate or growing EP film beneath, forming a strongly adhered, dense and flat EP layer. Ramping the reactor temperature during deposition from 290 °C to 350 °C conferred the microstructure, while the smallest particles formed at the highest temperature of the ramping cycle were able to settle atop and in between larger particles already present on the growing film; the result is the protection of the nanoscopic structure by the larger microscopic features, enhancing the robustness of the film while conserving the superhydrophobicity enhancement of the hierarchical structure. The three-layered films described were carried forward for further testing herein.

3.4 Environmental stability of three-layered EP/PDMS films

Stability testing of the three-layered films was carried out under the impact of 3000 water droplets (~ 15 μL) dropped from different heights (20 cm - 80 cm) onto the horizontal sample. Fig. 4(a) illustrates the effect on the water contact angle and sliding angle of increased drop height, with CA and SA measurements taken at 20 cm intervals up to a maximum of 80 cm. Even at the greatest drop height, the CA still exceeded 158° while the SA remained below 1°. The surface structure of the EP/PDMS film after the impact of 3000 such water droplets from 80 cm height is shown in Fig. 4(b). It is apparent that the film retained its microstructure to a sufficient degree that resilience to water droplet impact can be claimed. The resilience was due to a combination of the physical robustness of the bond between EP clusters and the glass, and the low surface energy of the PDMS which had a water-repellent effect.

In further testing, water droplets were replaced by sand grains. 20 g of sand grains were again dropped from different heights (20 cm - 80 cm), but this time onto a slightly tilted surface as can be seen in the online supplementary Video S3. Subsequent measurements of droplet CAs and SAs investigated the effect had on superhydrophobicity. It can be seen from Fig. 4(c) that superhydrophobicity was slightly compromised with increasing dropping height; CA fell to 155° while SA increased to 2° at 80 cm drop height, the effect of which on surface microstructure shown in Fig. 4(d). The film still retained its roughness with micro and nano spherical particles, which bodes well for the lifetime of these devices in the longer term under everyday stresses.

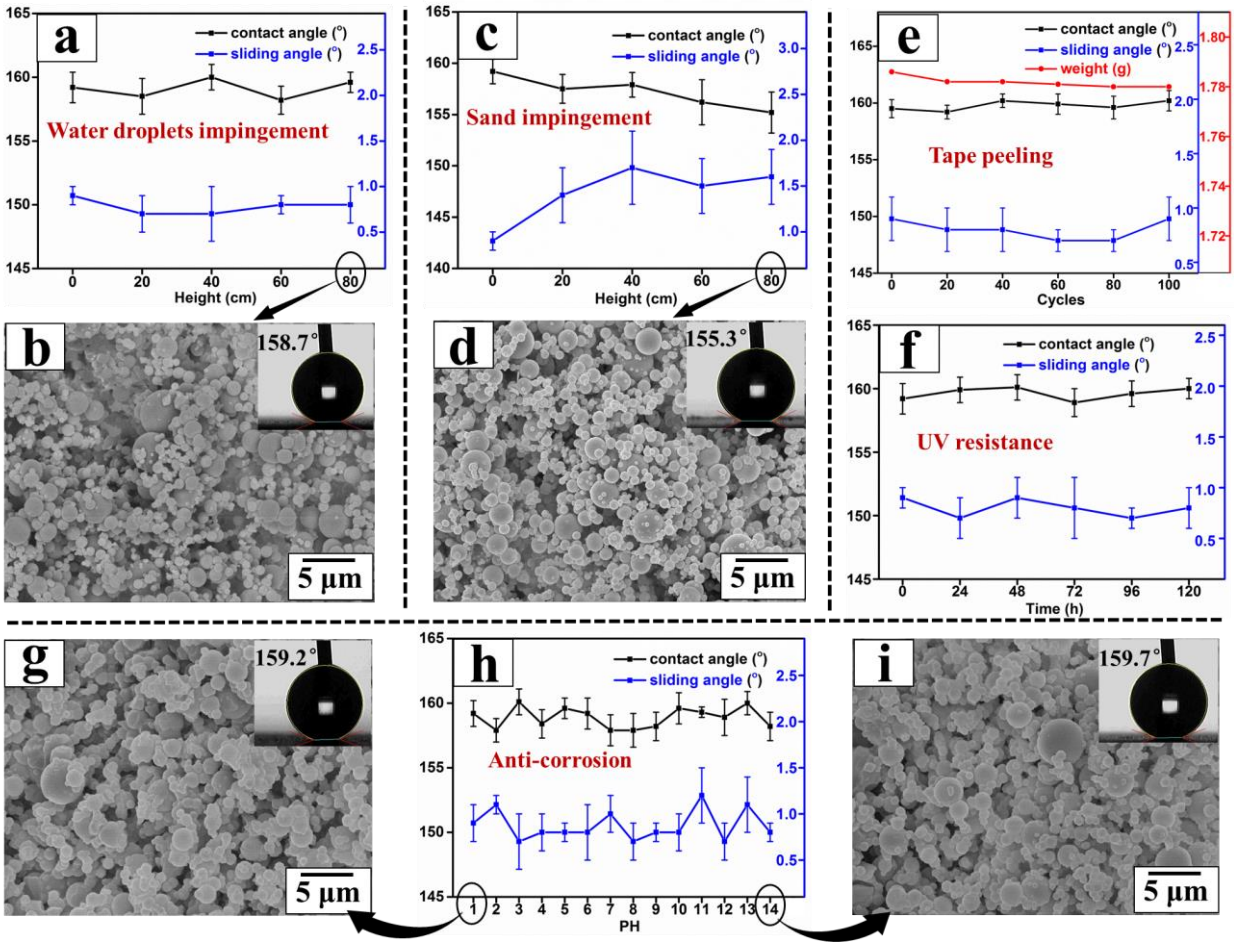

Fig. 4. Contact angles, sliding angles and SEM images of the superhydrophobic EP/PDMS films after impingement of 3000 water droplets (~ 15 mL) (a) - (b) and 20 g sand grains (c) - (d) from different heights (20 cm - 80 cm); contact angles, sliding angles and weight of the sample films after tape peeling with different cycles (e); contact angles and sliding angles of the sample films after UV exposure (365 nm, 3.7 mW/cm^2) with different time (f); contact angles, sliding angles and SEM images of the sample films after pH testing (pH = 1 - 14) for 72 h (g) - (i).

The adhesion between films and substrates is one of the most important factors for the large-scale practical applications.[45] Here, tape peeling test was used to investigate the adhesion between the EP/PDMS films and the substrates. Fig. 4(e) shows the CAs, SAs and weight of the superhydrophobic EP/PDMS film after multiple cycles (20 - 100) of tape peeling tests. It can be found that the EP/PDMS films exhibited consistent superhydrophobicity (CAs above 158° and SAs <1°) even after 100 cycles of tape peeling. Moreover, the weight of the sample film only reduced 0.006 g (from 1.786 g to 1.780 g) which suggests that the EP/PDMS films have strong adhesion to the substrate.

In order to test the UV resistance of the superhydrophobic EP/PDMS surfaces, the samples were exposed to UV light (365 nm, 3.7 mW/cm^2) for 120 h at room temperature, and CAs and SAs of the resulting EP/PDMS surfaces were measured after each 24-hour period as shown in Fig. 4(f). It was observed that the wettability of EP/PDMS surfaces exhibited consistent superhydrophobicity with a contact angle of 159° and a sliding angle <1° after irradiation for 120 h, showing a superior

UV-stability. This is due to the excellent UV stability of epoxy resin and PDMS which could not be easily damaged by the UV light.

Sufficient resistance to corrosion of the superhydrophobic film is required for its application to the outdoor environment. Corrosion testing was performed by immersing the films for 72 h in hydrochloric acid and sodium hydroxide solutions spanning pH = 1 to 14. CAs and SAs were used as a metric for corrosion resistance and are shown in Fig. 4(h). Wettability of samples appeared largely unaffected by the testing. The CAs of the surfaces were still >159° and SAs were <1° even after soaking at pH = 1 and pH = 14 for 72 hours. The resulting surface morphologies after soaking at pH = 1 and pH = 14 observed by SEM are shown in Fig.4 (g) and Fig.4 (i). It is evident that the surface morphology was largely unchanged by extreme pH environments due to the strong intrinsic corrosion resistance of EP and PDMS alongside the protection conferred by superhydrophobicity, which would have reduced contact between the film surface and solution.

3.5 Self-cleaning of superhydrophobic surface

Activated carbon powder and some dye powder including Congo red, Titan yellow and Trypan blue, as the representative examples of contaminant, were used to test the self-cleaning property of the three-layered superhydrophobic EP/PDMS surface for removing dust. Fig. 5(a) - (d) show that activated carbon powder and the dye powder were dispersed on the tilted superhydrophobic EP/PDMS surface, followed by the addition of water droplets from above. The artificial dirt was readily collected by the incident droplets and rolled off the films, thus demonstrating self-cleaning. Moreover, in order to test the self-cleaning property with corrosive liquid, aqueous HCl (pH = 1) and NaOH (pH = 14) were used in a similar manner to the plain water droplets in the previous test. Samples still exhibited self-cleaning under strongly corrosive liquid, as shown in Fig. 5(e) and (f). Aqueous dyes, including Congo red, Titan yellow and Trypan blue, were chosen to investigate the self-cleaning property of the superhydrophobic EP/PDMS surface for the dirty liquid. Fig. 5(g) - (h) illustrate ready wetting of untreated glass by the aqueous dye, while the superhydrophobic EP/PDMS surface appeared dry and free of staining.

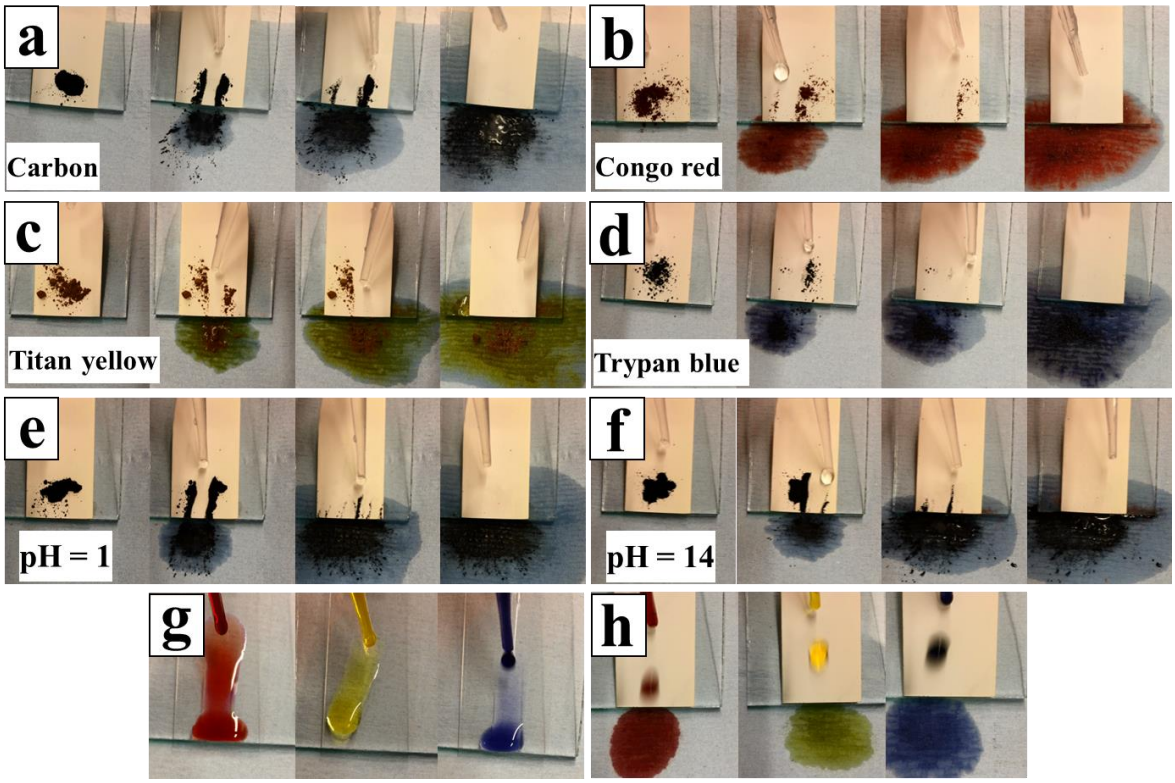

Fig. 5. Self-cleaning properties of the superhydrophobic EP/PDMS surface; water drops collect carbon, Congo red, Titan yellow and Trypan blue contaminants dispersed across sample surfaces (a) - (d); hydrochloric acid solution (pH = 1) (e) and sodium hydroxide solution (pH = 14) (f) used for the same; dropping aqueous solutions of the dyes onto bare glass (g) and superhydrophobic EP/PDMS surface (h).

4. Conclusion

Robust superhydrophobic films of an epoxy resin/polydimethylsiloxane composite with hierarchical micro/nano-structured particles were prepared on glass substrates using a facile dynamic temperature deposition by aerosol-assisted chemical vapour deposition. The films demonstrated water droplet contact angles up to 160° and excellent surface mechanical stability. Wear testing demonstrated that, after rigorous abrasion testing with sandpaper, the film still retained superhydrophobic performance. Meanwhile, the films also showed excellent stability for UV/wear resistance, tape peeling, anti-corrosion and self-cleaning properties. Dynamic temperature deposition resulted in small nanoparticles being embedded into and well protected by micron structures. Upon building multiple layers, the periodic micro-nano scaled structures significantly improved the mechanical property of the coating compared with the coatings only with nanoparticles even within the same film thickness. This method for epoxy resin deposition is cheap and straightforward, promising a route to larger-scale robust superhydrophobic coating fabrication, while the approach of periodically multi-layered micro-nano structures opens up the field to a huge variety of potential material combinations in superhydrophobic coatings design.

Supporting Information

Videos showing the bounce dynamics and robustness of the EP/PDMS films. This material is

available free of charge via the Internet at http://pubs.acs.org.

Acknowledgment
This work is financially supported by the General Program of Natural Science Foundation of China (51377177). NSG Pilkington Glass Ltd. and the EPSRC are thanked for studentship funding for S. C. Dixon through the M^3S Doctoral Training Centre at UCL (grant EP/G036675). A. Zhuang thanks for the funding from China Scholarship Council (CSC). Y. Lu acknowledges the support from EPSRC project EP/N024915/1.

References

(1) Barthlott, W.; Neinhuis, C. Purity of the Sacred Lotus, or Escape from Contamination in Biological Surfaces. *Planta* **1997**, *202*, 1–8.
(2) Denny, M. Water-Repellent Legs of Water Striders. *Science (80-.).* **2008**, 7013.
(3) Lee, W.; Jin, M. K.; Yoo, W. C.; Lee, J. K. Nanostructuring of a Polymeric Substrate with Well-Defined Nanometer-Scale Topography and Tailored Surface Wettability. *Langmuir* **2004**, *20*, 7665–7669.
(4) Kamegawa, T.; Yamashita, H. Chapter 4. Superhydrophilic and Superhydrophobic Thin Film Type of Photocatalysts with Self-Cleaning Properties. *Self-cleaning Coatings* 86–104.
(5) Sojoudi, H.; Wang, M.; Boscher, N. D.; McKinley, G. H.; Gleason, K. K. Durable and Scalable Icephobic Surfaces: Similarities and Distinctions from Superhydrophobic Surfaces. *Soft Matter* **2016**, *12*, 1938–1963.
(6) Cho, E.-C.; Chang-Jian, C.-W.; Chen, H.-C.; Chuang, K.-S.; Zheng, J.-H.; Hsiao, Y.-S.; Lee, K.-C.; Huang, J.-H. Robust Multifunctional Superhydrophobic Coatings with Enhanced Water/oil Separation, Self-Cleaning, Anti-Corrosion, and Anti-Biological Adhesion. *Chem. Eng. J.* **2017**, *314*, 347–357.
(7) Chu, Z.; Seeger, S. Superamphiphobic Surfaces. *Chem. Soc. Rev.* **2014**, *43*, 2784–2798.
(8) Chen, F.; Song, J.; Lu, Y.; Huang, S.; Liu, X.; Sun, J.; Carmalt, C. J.; Parkin, I. P.; Xu, W. Creating Robust Superamphiphobic Coatings for Both Hard and Soft Materials. *J. Mater. Chem. A* **2015**, *3*, 20999–21008.
(9) Darmanin, T.; Guittard, F. Recent Advances in the Potential Applications of Bioinspired Superhydrophobic Materials. *R. Soc. Chem.* **2013**, *0*, 1–3.
(10) Long, J.; Pan, L.; Fan, P.; Gong, D.; Jiang, D.; Zhang, H.; Li, L.; Zhong, M. Cassie-State Stability of Metallic Superhydrophobic Surfaces with Various Micro/Nanostructures Produced by a Femtosecond Laser. *Langmuir* **2016**, *32*, 1065–1072.
(11) Wu, X.; Fu, Q.; Kumar, D.; Ho, J. W. C.; Kanhere, P.; Zhou, H.; Chen, Z. Mechanically Robust Superhydrophobic and Superoleophobic Coatings Derived by Sol-Gel Method. *Mater. Des.* **2016**, *89*, 1302–1309.
(12) Chen, F. Z.; Xu, W. J.; Lu, Y.; Song, J. L.; Huang, S.; Wang, L.; Parkin, I. P.; Liu, X. Hydrophilic Patterning of Superhydrophobic Surfaces by Atmospheric-Pressure Plasma Jet. *Micro {&} Nano Lett.* **2015**, *10*, 105–108.
(13) Tripathi, S.; Maidul Haque, S.; Divakar Rao, K.; De, R.; Shripathi, T.; Deshpande, U.; Ganesan, V.; Sahoo, N. K. Investigation of Optical and Microstructural Properties of RF Magnetron Sputtered PTFE Films for Hydrophobic Applications. *Appl. Surf. Sci.* **2016**, *385*, 289–298.
(14) Su, C.; Li, Y.; Dai, Y.; Gao, F.; Tang, K.; Cao, H. Fabrication of Three-Dimensional Superhydrophobic Membranes with High Porosity via Simultaneous Electrospraying and

Electrospinning. *Mater. Lett.* **2016**, *170*, 67–71.
(15) Xiao, C.; Si, L.; Liu, Y.; Guan, G.; Wu, D.; Wang, Z.; Hao, X. Ultrastable Coaxial Cable-like Superhydrophobic Mesh with Self-Adaption Effect: Facile Synthesis and Oil/water Separation Application. *J. Mater. Chem. A* **2016**, *0*, 1–11.
(16) Matsubayashi, T.; Tenjimbayashi, M.; Manabe, K.; Kyung, K.-H.; Ding, B.; Shiratori, S. A Facile Method of Synthesizing Size-Controlled Hollow Cyanoacrylate Nanoparticles for Transparent Superhydrophobic/oleophobic Surfaces. *RSC Adv.* **2016**, *6*, 15877–15883.
(17) Rather, A. M.; Manna, U. Facile Synthesis of Tunable and Durable Bulk Superhydrophobic Material from Amine "Reactive" Polymeric Gel. *Chem. Mater.* **2016**, *28*, 8689–8699.
(18) Seo, K.; Kim, M.; Kim, D. H. Candle-Based Process for Creating a Stable Superhydrophobic Surface. *Carbon N. Y.* **2014**, *68*, 583–596.
(19) Latthe, S. S.; Rao, A. V. Superhydrophobic SiO2 Micro-Particle Coatings by Spray Method. *Surf. Coatings Technol.* **2012**, *207*, 489–492.
(20) Zhuang, A.; Yang, L.; Liao, R.; Guo, C.; Zuo, Z.; Yuan, Y. A Simple Method to Make Mechanically Robust, Adhesive and Superhydrophobic Surface Based on Epoxy Resin. *J. Coatings Technol. Res.* **2015**, *12*, 609–615.
(21) Wang, P.; Chen, M.; Han, H.; Fan, X.; Liu, Q.; Wang, J. Transparent and Abrasion-Resistant Superhydrophobic Coating with Robust Self-Cleaning Function in Either Air or Oil. *J. Mater. Chem. A* **2016**, *4*, 7869–7874.
(22) Wang, L.; Gong, Q.; Zhan, S.; Jiang, L.; Zheng, Y. Robust Anti-Icing Performance of a Flexible Superhydrophobic Surface. *Adv. Mater.* **2016**, *28*, 7729–7735.
(23) Hoshian, S.; Jokinen, V.; Franssila, S. Novel Nanostructure Replication Process for Robust Superhydrophobic Surfaces. *Proc. IEEE Int. Conf. Micro Electro Mech. Syst.* **2016**, *2016–Febru*, 547–549.
(24) Gong, D.; Long, J.; Jiang, D.; Fan, P.; Zhang, H.; Li, L.; Zhong, M. Robust and Stable Transparent Superhydrophobic Polydimethylsiloxane Films by Duplicating via a Femtosecond Laser-Ablated Template. *ACS Appl. Mater. Interfaces* **2016**, *8*, 17511–17518.
(25) Lu, Y.; Sathasivam, S.; Song, J.; Crick, C. R.; Carmalt, C. J.; Parkin, I. P. Robust Self-Cleaning Surfaces That Function When Exposed to Either Air or Oil. *Science (80-.).* **2015**, *347*, 1132–1135.
(26) Si, Y.; Guo, Z.; Liu, W. A Robust Epoxy Resins @ Stearic Acid-Mg(OH)2 Micronanosheet Superhydrophobic Omnipotent Protective Coating for Real-Life Applications. *ACS Appl. Mater. Interfaces* **2016**, *8*, 16511–16520.
(27) Zhang, X.; Si, Y.; Mo, J.; Guo, Z. Robust Micro-Nanoscale Flowerlike ZnO/epoxy Resin Superhydrophobic Coating with Rapid Healing Ability. *Chem. Eng. J.* **2017**, *313*, 1152–1159.
(28) Atta, A. M.; Al-Lohedan, H. A.; Ezzat, A. O.; Al-Hussain, S. A. Characterization of Superhydrophobic Epoxy Coatings Embedded by Modified Calcium Carbonate Nanoparticles. *Prog. Org. Coatings* **2016**, *101*, 577–586.
(29) Hsu, C. P.; Chang, L. Y.; Chiu, C. W.; Lee, P. T. C.; Lin, J. J. Facile Fabrication of Robust Superhydrophobic Epoxy Film with Polyamine Dispersed Carbon Nanotubes. *ACS Appl. Mater. Interfaces* **2013**, *5*, 538–545.
(30) Liu, Y.; Lin, Z.; Lin, W.; Moon, K. S.; Wong, C. P. Reversible Superhydrophobic-Superhydrophilic Transition of ZnO Nanorod/epoxy Composite Films. *ACS Appl. Mater. Interfaces* **2012**, *4*, 3959–3964.
(31) Ponja, S.; Sathasivam, S.; Chadwick, N.; Kafizas, A.; Bawaked, S. M.; Obaid, A. Y.; Al-Thabaiti, S.; Basahel, S. N.; Parkin, I. P.; Carmalt, C. J. Aerosol Assisted Chemical Vapour Deposition of

Hydrophobic TiO2-SnO2 Composite Film with Novel Microstructure and Enhanced Photocatalytic Activity. *J. Mater. Chem. A* **2013**, *1*, 6271–6278.

(32) Dixon, S. C.; Sathasivam, S.; Williamson, B. A. D.; Scanlon, D. O.; Carmalt, C. J.; Parkin, I. P. Transparent Conducting N-Type ZnO:Sc – Synthesis, Optoelectronic Properties and Theoretical Insight. *J. Mater. Chem. C* **2017**, *5*, 7585–7597.

(33) Crick, C. R.; Gibbins, J. A.; Parkin, I. P. Superhydrophobic Polymer-Coated Copper-Mesh; Membranes for Highly Efficient Oil–water Separation. *J. Mater. Chem. A* **2013**, *1*, 5943.

(34) Crick, C. R.; Bear, J. C.; Kafizas, A.; Parkin, I. P. Superhydrophobic Photocatalytic Surfaces through Direct Incorporation of Titania Nanoparticles into a Polymer Matrix by Aerosol Assisted Chemical Vapor Deposition. *Adv. Mater.* **2012**, *24*, 3505–3508.

(35) Crick, C. R.; Parkin, I. P. A Single Step Route to Superhydrophobic Surfaces through Aerosol Assisted Deposition of Rough Polymer Surfaces: Duplicating the Lotus Effect. *J. Mater. Chem.* **2009**, *19*, 1074–1076.

(36) Dixon, S.; Noor, N.; Sathasivam, S.; Lu, Y.; Parkin, I. Synthesis of Superhydrophobic Polymer/tungsten (VI) Oxide Nanocomposite Thin Films. *Eur. J. Chem.* **2016**, *7*, 139–145.

(37) Zhuang, A.; Liao, R.; Dixon, S. C.; Lu, Y.; Sathasivam, S.; Parkin, I. P.; Carmalt, C. J. Transparent Superhydrophobic PTFE Films via One-Step Aerosol Assisted Chemical Vapor Deposition. *RSC Adv.* **2017**, *7*, 29275–29283.

(38) Wu, H.; Yang, Z.; Cao, B.; Zhang, Z.; Zhu, K.; Wu, B.; Jiang, S.; Chai, G. Wetting and Dewetting Transitions on Submerged Superhydrophobic Surfaces with Hierarchical Structures. *Langmuir* **2017**, *33*, 407–416.

(39) Hia, I. L.; Pasbakhsh, P.; Chan, E.; Chai, S. Electrosprayed Multi-Core Alginate Microcapsules as Novel Self-Healing Containers. *Nat. Publ. Gr.* **2016**, 1–8.

(40) Stuart, B. *Infrared Spectroscopy: Fundamentals and Applications*; 2004.

(41) Crick, C. R.; Parkin, I. P. Water Droplet Bouncing--a Definition for Superhydrophobic Surfaces. *Chem. Commun. (Camb).* **2011**, *47*, 12059–12061.

(42) Liu, Y.; Moevius, L.; Xu, X.; Qian, T.; Yeomans, J. M.; Wang, Z. Pancake Bouncing on Superhydrophobic Surfaces. *Nat. Phys.* **2014**, *10*, 515–519.

(43) Cassie, A. B. D.; Baxter, S. Wettability of Porous Surfaces. *Trans. Faraday Soc.* **1944**, *40*, 546.

(44) Yu, L.; Chen, G. Y.; Xu, H.; Liu, X. Substrate-Independent, Transparent Oil-Repellent Coatings with Self-Healing and Persistent Easy-Sliding Oil Repellency. *ACS Nano* **2016**, *10*, 1076–1085.

(45) Zhi, D.; Lu, Y.; Sathasivam, S.; Parkin, I. P.; Zhang, X. Large-Scale Fabrication of Translucent and Repairable Superhydrophobic Spray Coatings with Remarkable Mechanical, Chemical Durability and UV Resistance. *J. Mater. Chem. A* **2017**, *5*, 10622–10631.

A Table of Contents (TOC) graphic: